Fusion Reaction-Rate Measurements—Nova and NIF

R. A. Lerche

M. D. Cable

Introduction

Thermonuclear fusion can occur when laser energy compresses and heats a spherical capsule filled with deuterium (DD) or a deuterium–tritium (DT) mixture. A goal of the Inertial Confinement Fusion (ICF) Program is to achieve a compression of 1000 times liquid density at a temperature of ~10 keV for a plasma confined for ~100 ps.[1] During confinement, fuel atoms undergo fusion and release energy in the form of energetic charged particles, neutrons, and photons. We want to measure the fusion reaction rate as a function of time relative to the incident laser radiation because it is valuable information for researchers studying laser–target interactions. These measurements characterize the coupling of the drive energy to the target, the hydrodynamics of the capsule implosion, and the plasma conditions during peak emission. The fusion reaction rate, often referred to as "burn rate" or "burn history," is a sensitive indicator of our ability to accurately model energy transport between the laser and target.

The burn history for a target can be measured by monitoring the production rate of the fusion reaction products. At Nova, most measurements are made by recording the arrival time of 14-MeV neutrons produced in T(d,n)^{4}He fusion reactions using a fast (30-ps resolution) detector several centimeters from the target.[2] Since fusion products are nearly monoenergetic and the target's emission region is submillimeter in size, the recorded signal is the target burn history with a time-of-flight delay dependent on the target-to-detector distance.

At the future National Ignition Facility (NIF), it is unlikely that the target burn history can be measured with the direct neutron technique used at Nova. This is because the thermal motion of the reacting plasma ions causes a broadening of the neutron energy spectrum, which in turn causes a temporal spread in neutron flight time to a detector. The time spread increases with target-to-detector distance. At NIF, there will be an exclusion zone around the target to minimize damage to blast shields and optics caused by ablated material. At anticipated detector distances of 1 to 5 m, the resulting spread in the neutron arrival times will mask burn-history information. Gamma rays, however, are virtually unaffected by plasma temperature and have negligible temporal dispersion at a distant detector. For these reasons, we are investigating techniques that use fusion gamma rays to measure burn history.

This article begins with a review of detector system characteristics required for making reaction-rate measurements. A description of the neutron-based measurement system implemented at Nova is followed with examples of reaction-rate measurements made for a variety of Nova targets. Finally, we discuss the challenge of measuring burn history at NIF and summarize current experiments associated with developing a gamma-ray-based technique to measure burn history.

Measurement Concept

One method for measuring the fusion reaction rate of an ICF target is to monitor the production rate of a fusion reaction product. Reactions available for DD- and DT-filled targets are

$$\mathrm{D + D \rightarrow\ ^3He\ (0.82\ MeV) + n\ (2.54\ MeV)}$$

$$\mathrm{D + D \rightarrow\ ^4T\ (1.01\ MeV) + p\ (3.02\ MeV)}$$

$$\mathrm{D + T \rightarrow\ ^4He\ (3.56\ MeV) + n\ (14.03\ MeV)}$$

$$\mathrm{D + T \rightarrow\ ^5He + \gamma\ (16.7\ MeV)}\quad ,$$

where the particle energy is indicated in parentheses. The spectrum for each fusion product is nearly monoenergetic. The charged particles are slowed by Coulomb interactions with plasma ions and electrons before leaving the target. Most neutrons and gamma rays, however, escape from the target without collision. Since the reaction region is submillimeter in size, both neutron and gamma-ray temporal distributions at points outside the target preserve burn history. For this

reason, burn history may be measured with either a fast neutron or gamma-ray detector placed some distance away from the target. Since confinement times can be <100 ps, detectors with time resolutions of ~20 ps are desirable.

Temporal resolution for a neutron-based measurement is limited by the plasma ion temperature, the target-to-detector distance, and the detector thickness. Thermal motion of the reacting plasma ions causes a broadening of the neutron energy spectrum.[3] For neutrons leaving a target at the same instant, the energy spread causes a time spread in their arrival at a detector. The time spread Δt_e, which is proportional to distance, is given by $\Delta t_e = 1.22\sqrt{T} \times d$ for DT neutrons and $\Delta t_e = 7.88\sqrt{T} \times d$ for DD neutrons, where Δt_e is in ps, ion temperature T is in keV, and target-to-detector distance d is in cm. The detector must be placed close to the target to keep the time spread small. For example, to keep Δt_e below 20 ps for a 1-keV plasma requires d <16.4 cm for DT neutrons and <2.6 cm for DD neutrons.

A neutron detector must also be thin to achieve 20-ps response. In a detector, there is an uncertainty about the exact point of neutron interaction, and a corresponding uncertainty in the instant of the interaction. The uncertainty Δt_x is proportional to the detector thickness Δx and is given by $\Delta t_x = \Delta x / v_n$, where v_n is the speed of the neutron. Thus, to achieve a 20-ps response requires Δx <1 mm for DT neutrons and <0.4 mm for DD neutrons.

The less restrictive requirements of DT neutrons on target-to-detector distance and detector thickness are advantages for selecting DT fuel over DD fuel for making burn-history measurements. Furthermore, the larger fusion cross section for DT reactions results in a neutron yield nearly 100 times greater than for a hydrodynamically equivalent DD-filled target, an important consideration when working with low-yield targets. The 16.7-MeV fusion gamma rays were never seriously considered for Nova reaction-rate measurements because of the low branching ratio (5×10^{-5}) for the reaction.[4,5] There simply were not enough gamma rays to make burn-history measurements at Nova.

30-ps Neutron Detector

A critical step in our effort to record reaction rates with 30-ps resolution was the development of a sensitive, high-speed neutron detector. RIC (radiation-induced conductivity) detectors,[6] the fastest available before we developed a streak-camera-based instrument, were not sensitive and fast enough. Coupled to a 7-GHz transient recorder, RIC detectors had an impulse response of 125 ps full-width half-maximum (FWHM) and required yields of $>5 \times 10^{10}$ DT neutrons for a reaction-rate measurement.

Our detector is based on the fast rise time of a commercially available plastic scintillator. A thin piece of BC-422[7] converts neutron kinetic energy into light. As neutrons pass through the scintillator, some of them have elastic collisions with hydrogen nuclei. The recoil protons quickly transfer their kinetic energy to luminescent sites in the scintillator. For BC-422 the light output has a rise time <20 ps and a decay time of ~1.2 ns. The temporal distribution of the emitted light is the convolution of the neutron temporal distribution with the scintillator response. Burn-history information is encoded in the leading edge of the light pulse. A fast optical streak camera (<15 ps FWHM) records the signal.

The detector is the result of three technology advances. First we developed a detector concept based on the fast rise time of a plastic scintillator. At that time, the fastest plastic scintillators had nanosecond decay times and were believed to have rise times >100 ps, hardly fast enough for 30-ps measurements. Second, an experimental search for a fast-rise-time scintillator using a pulsed electron beam at the LLNL linac identified NE-111 (BC-422) as a potential candidate.[8] Later experiments at Nova with short bursts of x rays generated by irradiating gold disk targets with 20-ps-wide laser pulses demonstrated the scintillator rise time to be <20 ps.[9] Third, we discovered that our streak camera could be operated with a wide input slit without losing temporal resolution.[10] Wide slit operation allowed us a tenfold increase in system sensitivity by using a 1-mm-wide slit rather than the more typical 100-μm-wide slit used with other streak cameras.

Figure 1 shows the scintillator configuration. A 6-mm-diam, 1-mm-thick piece of BC-422 is housed in a Hevimet

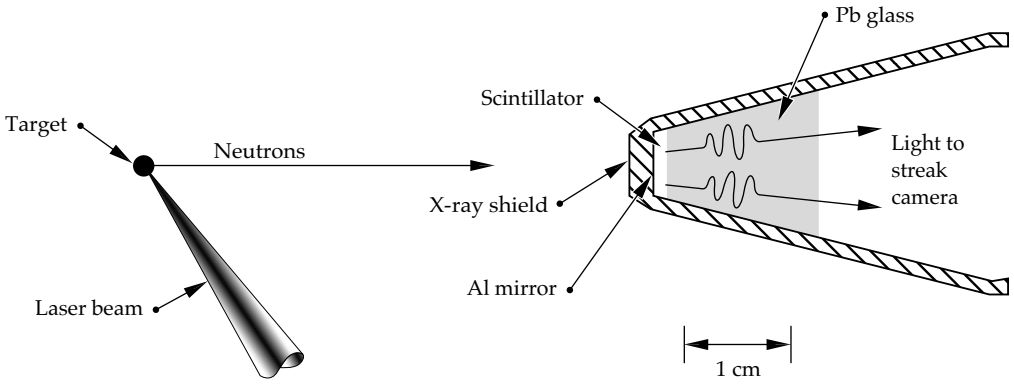

FIGURE 1. Detector nose cone configuration. Scintillator must be thin and close to the target to control temporal dispersion. (08-00-0896-1852pb01)

(90% tungsten) nose cone. The front of the nose cone, which is 3 mm thick, shields the scintillator from target x rays, scattered laser light, and target debris. A thin Al layer deposited on one surface of the scintillator acts as a mirror to double the light output directed towards the streak camera. A piece of Pb glass shields the back side of the scintillator from scattered x rays.

The detector system, which is called the NTD (for neutron timing diagnostic), features a nose cone assembly that can be positioned between 2 and 50 cm from the target. An achromatic $f/2$ zoom lens relays the scintillator image along a 4-m optical path to the S-20 photocathode of the streak camera located outside the vacuum chamber. Lens coupling produces minimal temporal dispersion. In contrast, using 4 m of graded-index optical fibers would produce ~80 ps of dispersion for the 350- to 450-nm scintillator light. Baffling and a light shield prevent scattered laser light from entering the lens system. Scintillator light passes through a glass window at the vacuum chamber wall. Components inside the chamber can operate at either vacuum or atmospheric pressure. The streak camera image is recorded with a charge-coupled device (CCD) camera. The relatively long distance between target and streak camera is an advantage of this configuration. Background caused by target x rays and neutrons interacting with the streak camera and the CCD decreases inversely with the square of the distance from the target.

Besides recording a neutron-induced signal, the streak camera also records an optical fiducial signal to provide an absolute time base. The Nova facility generates a 100-ps, 0.53-μm, optical timing pulse that is split and distributed to various diagnostic instruments via optical fibers. We insert a 527-ps etalon into its path to form a series of evenly spaced pulses. The first pulse provides an absolute timing reference required to temporally relate the neutron signal to the laser power recorded with other streak cameras with ±10-ps precision.[11] The pulse train provides a calibration check for the streak camera time base. The optical fiducial amplitude, timing, and pulse shape are easily controlled because they are independent of target type, incident laser energy, and target-to-detector distance. This is not the case when target-generated x rays are used as the fiducial.

Excellent data have been recorded with the NTD. Figure 2(a) shows an image recorded with the scintillator 2 cm from a low-yield target producing 6.7×10^8 DT neutrons. Figure 2(b) shows image exposure versus time averaged across the spatial extent of the neutron signal. Streak camera flat-field and time-base corrections are included in the signal processing. Information about the target burn history is encoded in the leading edge of the pulse.

We obtain the shape of the neutron temporal distribution by deconvolving the effect of the scintillator decay rate from the recorded neutron signal. The result, which is approximately the derivative of the recorded signal, actually represents the convolution of the target burn history with the streak camera response and the derivative of the scintillator rise time. Since the rise time and camera response are both <20 ps, the deconvolved signals are a good representation of the fusion reaction rate. The quality of each deconvolution is checked by comparing the recorded signal with the convolution of the burn history and the exponential decay of the scintillator.

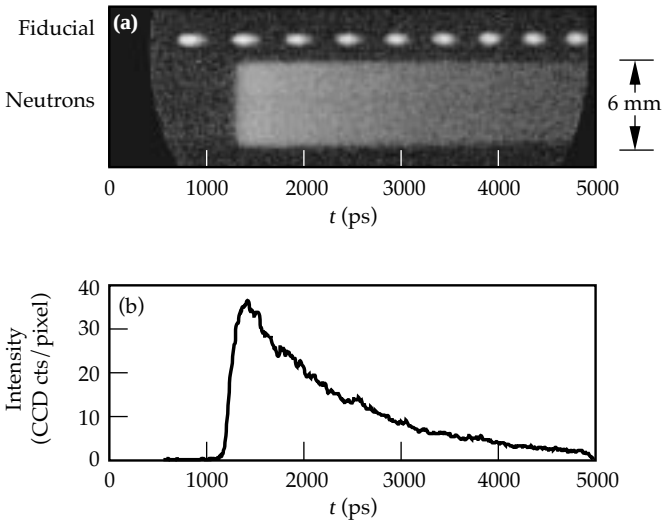

FIGURE 2. Neutron signal. (a) Streak camera image for a target producing 6.7×10^8 DT neutrons. (b) Average neutron signal intensity vs time. Burn history is encoded in the leading edge of the pulse. Pulse tail shows the characteristic decay of the scintillator. The complete burn history for this data is shown in Fig. 3(b). (08-00-0896-1853pb01)

Nova Reaction-Rate Measurements

Reaction-rate measurements with 30-ps resolution have been made for a variety of Nova targets whose DT yields ranged from 10^8 to 3.6×10^{13} neutrons. Measurements have also been made for targets with DD neutron yields between 10^9 and 10^{11}, but with temporal resolutions of ~50 ps. In this section, examples of burn histories for several different target types are presented. The intent of this section is to demonstrate the variety in burn-history signatures, and not to present a detailed examination of the performance of any particular target.

Direct-drive glass-microballoon targets are used for instrument development and calibration at Nova. Burn history is affected by target diameter, fill pressure, and wall thickness along with laser power and beam focusing. Diameters for microballoon targets range from 360 to 1500 μm, fill pressures from 10 to 100 atm, and wall thicknesses from 2 to 8 μm. High-yield targets (>10^{12} DT neutrons) typically have diameters >900 μm and are irradiated with temporally flat laser pulses 1 or 1.5 ns long. These targets typically have a burn duration between 175 and 250 ps (FWHM) and an emission time between 700 and 1500 ps after the leading edge of the laser pulse.

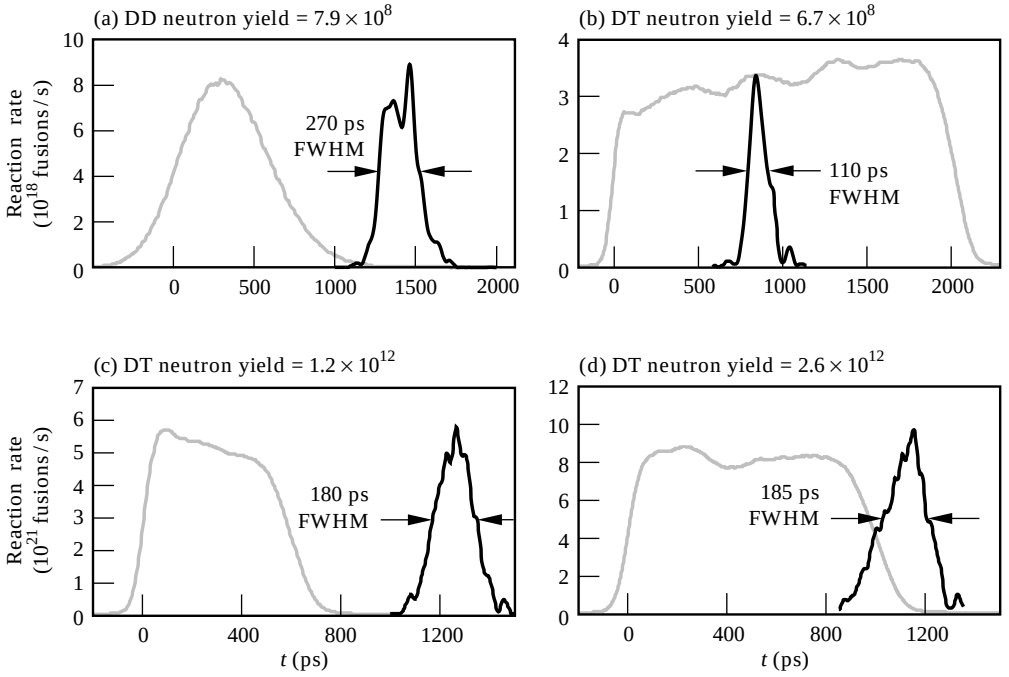

FIGURE 3. Reaction rates for four glass microballoon targets irradiated directly with 0.351-μm light. The black curves represent the reaction-rate history; the gray curves show the shape of the laser-power history. The target diameter/wall thickness, fill pressure, and incident laser energy for each experiment are (a) 360 μm/6 μm, 25 atm DD fuel, 15 kJ; (b) 360 μm/6 μm, 25 atm DT fuel, 20 kJ; (c) 800 μm/3 μm, 50 atm DT fuel, 11 kJ; and (d) 1000 μm/3 μm, 50 atm DT fuel, 22 kJ. (08-00-0896-1854pb01)

A small (360-μm) microballoon can have a burn duration as short as ~100 ps and an emission time as early as 500 ps after the leading edge of the laser pulse. Reaction history for microballoons is usually smooth but often shows an asymmetry of either a slow rise time or a slow fall time. Generally, larger, higher-pressure targets tend to burn later.

In July 1995, burn-history measurements provided the information needed to increase Nova's maximum yield from 2.1×10^{13} to 3.6×10^{13} neutrons. It was observed that neutron emission for large diameter (>1300 μm), thin-walled targets irradiated with 1-ns square pulses was occurring around 1400 ps, well after the laser pulse turned off. By changing to a 1.5-ns pulse with the same power, yield was immediately increased nearly twofold. Figure 3 shows the burn history for several microballoon targets along with the power history of the laser drive.

Our program has devoted significant effort to developing, designing, characterizing, and understanding indirect-drive targets. Fuel capsules for these targets are typically smaller diameter (360 μm) than direct-drive capsules, and are compressed to a higher convergence ratio at a lower temperature. Most indirect-drive capsules use deuterium fuel in a plastic capsule and produce yields between 10^7 and a few 10^9 DD neutrons. Reasonable burn-history measurements can only be made when DD yields are above 10^9, and signal quality for these low-yield targets depends very strongly on the background signal induced by x-ray emission from the target. Capsules in indirect-drive targets filled with DT fuel produce yields from 10^9 to over 10^{11}. Burn duration for these targets range from 50 to 125 ps. Two examples are shown in Fig. 4. Figure 4(a) is for a high-convergence implosion of a DT-filled glass capsule (from the HEP1 series of

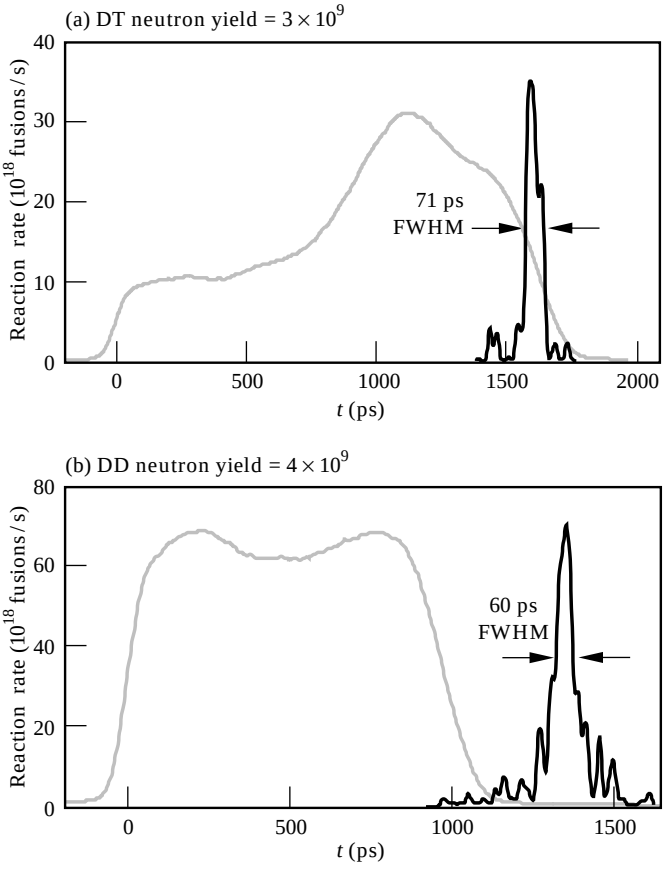

FIGURE 4. Reaction rates for two indirectly driven targets irradiated with 0.351-μm light. The black curves represent the reaction-rate history, the gray curves show the shape of the laser-power history. The type of target and its inner/outer diameters, fill pressure, and incident laser energy for each experiment are (a) glass capsule with CH layer, 180 μm/240 μm, 100 atm DT fuel, 25 kJ, and (b) plastic ball with CH layer, 430 μm/520 μm, 50 atm DD fuel, 27 kJ. (08-00-0896-1855pb02)

experiments)[12,13]; Fig. 4(b) is for an implosion of a DD-filled, Br-doped plastic capsule (from the HEP4 series of experiments)[14]. The reaction rate for the HEP4 capsule approaches the 50-ps resolution limit for DD neutrons in a 1-mm-thick detector.

Figure 5 shows the burn history for a special target used to resolve a "bang time" calibration issue with another detector used at Nova. The burn-history details differ significantly from the previous examples. The most important target characteristic is the very short time delay between laser irradiation and the start of neutron emission. Targets were 1-mm-by-2-mm, 320-μm-thick pieces of deuterated polystyrene (C_8D_8), each with a 400-μm hole drilled through it. Tritium was added to the targets by placing them in a tritium gas where tritium atoms replaced deuterium atoms. Targets were irradiated with 2.7 kJ of 0.351-μm laser light delivered in simultaneous 90-ps pulses from each of the ten Nova laser beams. Beams were set at best focus halfway down the inner wall of the hole and evenly spaced at five points around the circumference, one beam from each side of the target focused to each point. DT yields of 5×10^9 neutrons were high enough to produce good burn-history measurements. Low-level neutron emission was observed when the laser pulse reached 50% of its peak power. Significant neutron emission began 70 ps later and lasted ~300 ps. The other detector showed neutron emission starting ~250 ps earlier, before the start of the laser pulse.

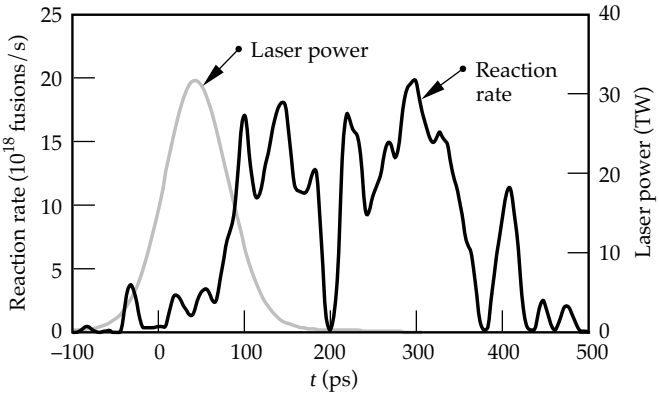

FIGURE 5. Reaction rate for a polystyrene target with a 400-μm-diam hole. There is almost no delay between laser irradiation and the start of neutron emission. (08-00-0896-1856pb01)

A serious concern for direct-drive ICF implosions is the early time "imprint" of laser-beam nonuniformity that can seed Rayleigh–Taylor instability growth. Los Alamos National Laboratory personnel recently conducted Nova experiments in their investigation of foam buffering as a way to reduce the effect of imprinting.[15] Figure 6 shows burn histories recorded for the three different target configurations irradiated in this study:

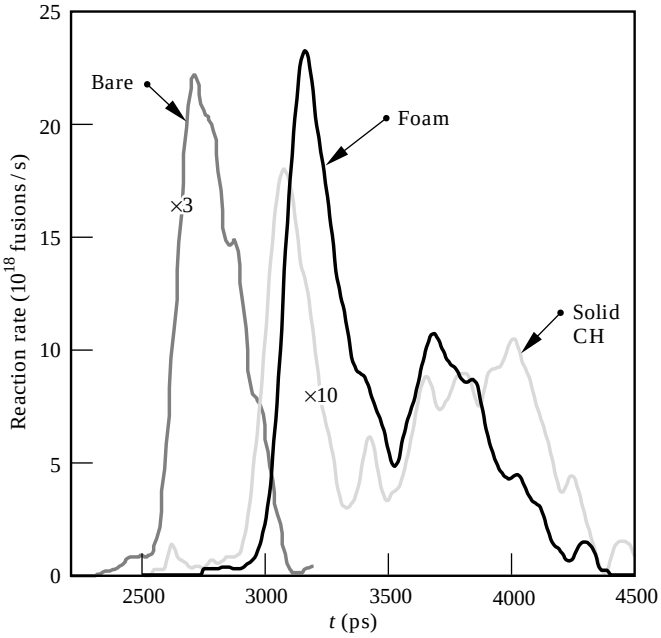

FIGURE 6. Reaction rates for three target types: a "bare" glass microballoon, a CH-foam-coated target, and a solid-CH-covered target. Laser power was delivered at a wavelength of 0.527-μm in 1.5-ns flat-topped pulses. Laser irradiation ends ~1.5 ns before fusion begins. The time base is relative to the beginning of the 1.5-ns wide laser pulse. The "bare" and "solid CH" curves have been scaled by factors of three and ten, respectively. (08-00-0896-1857pb01)

- A 1300-μm-diam, "bare" glass microballoon with a 4-μm-thick wall filled with 20 atm of DT fuel.
- Targets coated with a 200-μm-thick layer of 45-mg/cm^3 polystyrene (CH) foam.
- Targets covered with a 10-μm-thick layer of solid density CH.

Foam-coated targets were irradiated with 0.527-μm light at full Nova energy (34 kJ) delivered in a 1-ns flat-topped pulse. The bare microballoon and solid-CH-covered targets were irradiated at reduced energies of 9 kJ and 21 kJ, respectively, to better match implosion parameters with the foam-coated targets irradiated at 34 kJ. The bare microballoon had a single burn peak 290 ps FWHM. The peak is significantly delayed (~1.5 ns) from the peaks of bare microballoons irradiated under standard conditions. This delay is due to the large target diameter and low drive energy. Both the foam and solid-CH-covered targets show a narrow first peak followed by a broader second peak. Calculations suggest the first peak is caused by heating and compression of the first shock reaching target center and the second peak is from DT burn at the time of peak shell compression.

NIF Reaction-Rate Measurements

At the future NIF, fusion reaction rates cannot be measured with 30-ps resolution using the direct neutron-based technique employed at Nova. The target-to-detector spacing required by the NIF exclusion zone will cause

an excessive spreading in the neutron arrival times at the detector. Consider a very conservative example of a detector 1 m from a 4-keV plasma. The detector will see a temperature induced time spread of ~240 ps for DT neutrons. Since the plasma temperature and distance will likely be larger than these nominal values, this 240-ps time spread is a lower limit for neutron-based measurements at NIF. It is for this reason that we are investigating the use of gamma rays for making burn-history measurements.[16,17]

The increased neutron and gamma-ray yields expected for NIF targets should make a gamma-ray-based burn-history measurement possible. Measurements with gamma-rays are attractive because the gamma rays are virtually unaffected by the plasma temperature, have a large interaction cross section in many materials, and have no time dispersion at a distant detector. There are two possible sources of useful gamma rays in ICF experiments. The T(d,γ)^{5}He fusion reaction produces gamma rays with energies up to 16.7 MeV. The major disadvantage of this reaction is its low branching ratio of 5×10^{-5}. Another possible source of gamma rays is a small converter placed near the target, possibly built as a part of the target, that would convert neutrons to gamma rays through (n,γ) reactions. In this section, one detector concept and the first experimental observation of fusion gamma rays in an ICF experiment are described.[16] Much work remains to develop the sensitive, high-speed gamma-ray detector needed for NIF burn-history measurements.

Gamma-Ray Detector Concept

Figure 7 shows one concept for a gamma-ray-based burn-history measurement. Burning fuel isotropically emits fusion gamma rays, which travel radially outward from the compressed core of an ICF target. Some of the gamma rays interact with a two-stage converter to produce Cerenkov light. In the first converter stage, gamma rays produce forward-directed, relativistic electrons and positrons by Compton scattering and pair production. The charged particles move into a second converter stage, where they produce Cerenkov light. An optical system collects the Cerenkov light and relays it to a fast optical detector for recording.

Detector design will focus on providing an instrument with good time resolution ($\Delta t < 30$ ps) and sensitivity. The choice of low-Z or high-Z material for the first-stage gamma-ray converter determines whether the primary interaction is Compton scattering or pair production. For 16.7-MeV gamma rays, the interaction cross section for high-Z materials is ~100 times greater than it is for low-Z materials. Electron range, however, is much greater in low-Z materials. We estimate that about 15% of 16.7-MeV gamma rays incident on a high-Z converter several millimeters thick will produce electron-positron pairs that enter an adjacent Cerenkov converter.

The second converter stage determines the characteristics of the Cerenkov light. The threshold energy for production of Cerenkov radiation, the cone angle for its emission, and the number of photons emitted per centimeter of track length all depend on the index of refraction n of the converter material. Cerenkov light is produced in a material only when the speed of a charged particle exceeds the speed of light in that media. Thus, Cerenkov light is produced only when a particle's velocity relative to that of light in a vacuum β and n are such that $n\beta > 1$. Cerenkov radiation is emitted into a cone whose half angle θ relative to the direction of charged particle motion is given by $\cos\theta = (1/n\beta)$. The photon production rate in the visible spectrum (400 to 700 nm) is given by

$$\frac{dN}{dx} = 490\left(1 - \frac{1}{n^2\beta^2}\right) \text{photons/cm} \quad .$$

In Ref. 17, the secondary converter also forms part of the collection optics.

First Observation of Fusion Gamma Rays

We have conducted a set of direct-drive target experiments at Nova to assess our ability to detect fusion gamma rays. Yields from nominally 1-mm-diam DT-filled microballoons irradiated with 1-ns square

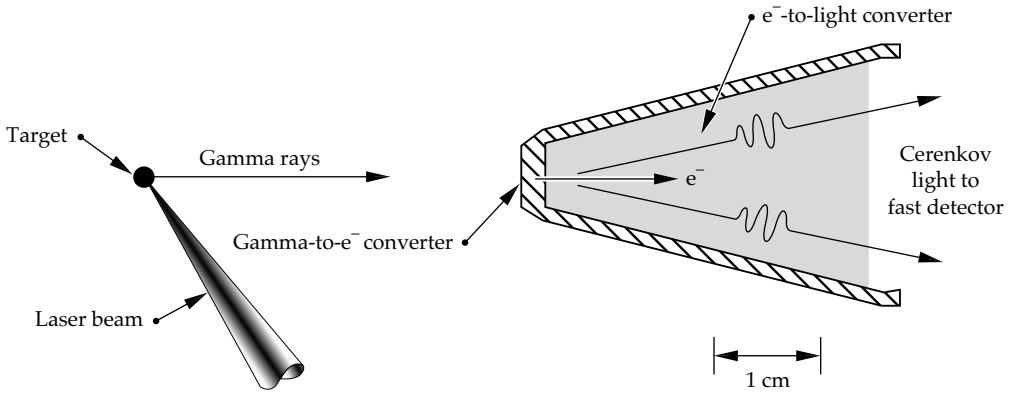

FIGURE 7. Cerenkov detector concept. A high-Z material converts target gamma rays to relativistic electrons and positrons that pass into a second converter stage. Since the charged particles are traveling faster than the speed of light in the second converter, Cerenkov light is produced. (08-00-0896-1858pb01)

pulses ranged from 10^{12} to 2×10^{13} neutrons. For these experiments, we adapted equipment normally used for our neutron burn-history measurements. The Hevimet (90% tungsten) nose cone (Fig. 1) acted as the first converter stage in which gamma rays interact primarily by pair production to produce electron-positron pairs. A 0.241-g/cm^3 silica aerogel filled the interior of the nose cone replacing the 1-mm-thick plastic scintillator and Pb glass. The aerogel acted as the second converter stage, converting relativistic electron energy into Cerenkov light. The aerogel, with $n = 1.06$, requires an electron energy >1.03 MeV to produce Cerenkov light. In our experiments, the high threshold level makes the detector relatively insensitive to target x rays and gamma rays from (n,γ) reactions near the target. A shallow cone angle of 19° allows some of the Cerenkov light to be collected by the $f/2$ optic and relayed to the streak camera. We estimate photon production at the rate of 53 photons per centimeter of track length. No modifications were made to the NTD optics to optimize collection of the Cerenkov light. Indeed, the optics, which were designed to pass scintillator light between 350 and 450 nm, have very poor transmission for Cerenkov light below 350 nm.

We observed weak gamma-ray signals in a set of target experiments with target-to-aerogel distances of 2, 3, and 4 cm (see Fig. 8). The signal for each experiment has a low-level gamma-ray pulse followed by a large 550-ps-wide pulse produced by 14-MeV target neutrons interacting with the 75-mm-diam $f/2$ optic of the telescope. The burn duration for these targets is nominally 200 ps FWHM. The neutron pulse width corresponds to the neutron transit time across the four-element optic ~2.5 cm behind the aerogel converter. The neutron signal amplitudes are normalized, temporally aligned, and overlaid. This allows us to easily observe the evolution of a small pulse to the left of the neutron peak. Its time relative to the neutron pulse changes with target-to-aerogel distance in a manner consistent with fusion gamma rays. Because the optic moves with the aerogel, a 1-cm increase in target-to-aerogel distance produces a 162-ps increase in the time separation between gamma-ray- and neutron-induced signals.

The streak camera simultaneously recorded a fiducial signal along with the aerogel signal. This allows us to determine the time of a gamma-ray signal relative to the laser power incident on a target. The time of the gamma-ray signal corresponds to the neutron emission time that we measure with a separate bang-time detector. For these targets, the nominal neutron emission time is at ~1 ns.

An additional experiment was performed with an aluminum nose cone replacing the Hevimet nose cone. In this configuration, the pair production cross section for 16.7-MeV gamma rays is reduced by a factor of 25 and the primary interaction mechanism changes to Compton scattering. The result (see Figure 9) is consistent with the small peak being caused by pair production in the high-Z nose cone. The gamma-ray signal observed with the Hevimet nose cone is not observed with the aerogel inside an aluminum nose cone. Also, with the substantially reduced shielding of the aluminum nose cone, there is no x-ray signal observed between the start of target irradiation and bang time, indicating a very low sensitivity to target x rays.

We believe these experiments are the first to detect fusion gamma rays emitted by T(d,γ)^{5}He reactions in ICF targets. The experimental evidence is consistent with this conclusion. First the change in time-of-flight

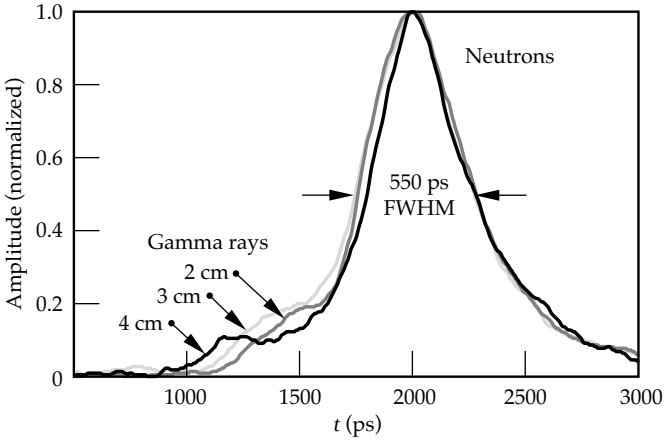

FIGURE 8. Aerogel signal intensity vs time for target-to-aerogel distances of 2, 3, and 4 cm. Neutron-induced signals from the first elements of the imaging optics are normalized, temporally aligned, and overlaid. Presented in this fashion, changes in the timing of the smaller gamma-ray signal relative to the neutron signal are easily observed. Time base is relative to incident laser power for the 4-cm gamma-ray data. (08-00-0896-1859pb01)

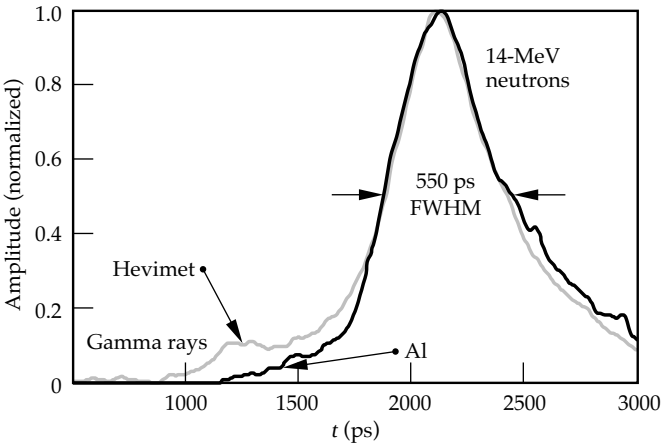

FIGURE 9. Aerogel signal intensity vs time for Hevimet and Al nose cones. The gamma-ray signal depends on high-Z converter material. (08-00-0896-1860pb01)

separation between gamma-ray and neutron pulses is consistent with the target-to-aerogel distances used. Second, the gamma-ray signals occur at the bang time of the target as determined with a separate neutron detector. Finally, the gamma-ray signal depends on the material used for the first converter stage in a manner consistent with pair production. The reduced shielding of the aluminum nose cone resulted in a decrease rather than an increase in the gamma-ray signal, indicating that the aerogel is a good threshold detector and that we are not detecting lower energy target x rays and gamma rays.

Conclusion

A neutron-based technique and a fast, sensitive neutron detector have been developed for measuring the fusion reaction rate of ICF targets. An absolute timing of ±20 ps and a temporal resolution of 30 ps have been achieved. Fusion reaction rates have been recorded for a variety of targets irradiated at the Nova Laser Facility. Target yields have ranged from 10^8 to 3.6×10^{13} DT neutrons.

Effort is now being directed towards developing a fast, sensitive burn-history detector based on fusion gamma rays. With a modification to our neutron detector, we have observed fusion gamma rays emitted from Nova high-yield targets, a significant first step in the development of a gamma-ray-based measurement. To obtain a temporal response <30 ps, we imagine the recording device of our final detector will remain a streak camera. Improved optical transmission of the second converter stage and imaging optics should enhance the signal by about a hundredfold. Based on the initial aerogel experiments, we predict a gamma-ray-based burn history can be made with a 25-cm-diam detector at the wall of the NIF chamber (5 m) when DT neutron yields are above ~10^{13}.

Acknowledgments

The following people contributed to the successful development of the fast neutron detector system: D. Phillion, G. Tietbohl, R. Ellis, J. Waldrep, J. Wass, G. Mant, R. Griffith, J. Hatch, J. Prior, N. Selchow, and D. Kumpf. The bang-time experiment with the deuterated polystyrene targets was designed and executed by T. Murphy. The initial gamma-ray experiments were done in collaboration with P. Dendooven. We also want to acknowledge S. Thomas for the development of the LLNL optical streak camera that made this work possible.

Notes and References

1. J. D. Lindl, R. L. McCrory, and E. M. Campbell, *Phys. Today* **45**, pp. 32–40 (1992); J. D. Lindl, *Phys. Plasmas* **2** (11), (1995).
2. R. A. Lerche, D. W. Phillion, and G. L. Tietbohl, *Rev. Sci. Instrum.* **66**(1), pp. 933–935 (1995).
3. H. Brysk, *Plasma Phys*. **15**, pp. 611–617 (1973).
4. F. E. Cecil and F. J. Wilkinson, III, *Phys. Rev. Lett.* **53**, pp. 767–770 (1984).
5. J. Kammeraad, J. Hall, K. E. Sale, C. A. Barnes, S. E. Kellogg, and T. R. Wang, *Phys. Rev. C* **47**(1), pp. 29–35, (1993).
6. D. R. Kania, S. M. Lane, and S. G. Prussin, *Appl. Phys. Lett.* **53** (20), pp. 1988–1989 (1988).
7. Bicorn Corp., Newbury, OH.
8. W. R. Graves, D. R. Slaughter, and R. A. Lerche, *Laser Program Annual Report 84,* pp. 5-64–5-65, Lawrence Livermore National Laboratory, Livermore, CA, UCRL-50021-84 (1985).
9. R. A. Lerche and D. W. Phillion, *Conference Record of the 1991 IEEE Nuclear Science Symposium and Medical Imaging Conference,* Vol. I, pp. 167–170, (IEEE, Piscataway, NJ, 91CH3100-5 1991).
10. R. A. Lerche and R. L. Griffith, "Resolution Limitations and Optimization of LLNL Streak Camera Focus," in *High-Speed Photography, Videography, and Photonics V*, H. C. Johnson, Ed., (SPIE —International Society for Optical Engineering, Bellingham, WA, 1988; *Proc. SPIE* **832**), pp. 266–274.
11. R. A. Lerche, "Timing Between Streak Cameras with a Precision of 10 ps," in *Ultrahigh- and High-Speed Photography, Videography, Photonics, and Velocimetry '90: Eighth in a Series,* L. L. Shaw, P. A. Jaanimagi, B. T. Neyer, Eds. (SPIE—International Society for Optical Engineering, Bellingham, WA, 1990; *Proc. SPIE*, **1346**) pp. 376–383.
12. M. D. Cable et al., *Phys. Rev. Lett*. **73**, pp. 2316–2319, (1994).
13. S. P. Hatchet et al., *ICF Quarterly Report* **5**(4), pp. 226–231, Lawrence Livermore National Laboratory, Livermore, CA, UCRL-LR-105821-95-4.
14. O. L. Landen et al., *ICF Quarterly Report* **5**(4), pp. 271–280, Lawrence Livermore National Laboratory, Livermore, CA, UCRL-LR-105821-95-4.
15. R. G. Watt et al., "Foam-Buffered Spherical Implosions at 527 nm," submitted for publication in *Phys. Plasmas.*
16. R. A. Lerche, "ICF Burn-History Measurements Using 17-MeV Fusion Gamma Rays," *12th International Conference on Laser Interaction and Related Plasma Phenomena, AIP Conference Proceedings* **369** Part 1, pp. 527–532 (1995).
17. K. P. Lewis, M. J. Moran, J. Hall, and M. Graser, *Rev. Sci. Instrum.* **63**(3), pp. 1988–1990 (1992).